51st IEEE Conference on Decision and Control
December 10-13, 2012. Maui, Hawaii, USA

Systematically Manipulating T-Cell Signaling Dynamics via Multiple Model Informed Open-Loop Controller Design*

Jeffrey P. Perley, Judith Mikolajczak, Vu C. Dinh, Marietta L. Harrison, Gregery T. Buzzard, and Ann E. Rundell

Abstract—**A multiple-model approach to open-loop control of T-cell signaling pathways is presented. Mathematical models of the T-cell signaling pathway are used to inform the controller design. The proposed framework employs a model predictive control strategy to reduce the computational complexity of the open loop control problem. Predictions from each model are weighted using adaptive Akaike weights that are iteratively computed for each controller update step based upon the most relevant training data subsets. This process accounts for the fact that models differ in their ability to accurately reflect the system dynamics under different experimental conditions. The algorithm is evaluated *in silico* and simulations demonstrate how the model weighting strategy more effectively manages the inaccuracies of any single model. Furthermore, the multiple-model control strategy is evaluated *in vitro* to direct T-cell signaling. The controller-derived input sequence successfully drives the relative concentration of phosphorylated Erk along the desired trajectory when implemented in the laboratory.**

I. Introduction

T lymphocytes (T cells) are an integral part of the human body's natural defense against the threats of invading pathogens and cancerous cells. Engagement of T cell receptors (TCRs) immediately initiates intracellular signal transduction pathways resulting in the activation of transcription factors that ultimately direct the cell's action. During this process, manipulations to the early signaling events within the transduction pathways can alter the cell's response through changes to the active transcription factor profile. Traditional biochemical assays can monitor only a limited number of signaling molecules and do not support real-time observations. As a result, open-loop control provides a suitable tool for designing systematic manipulations to obtain desired signaling responses.

Successful open-loop controller design requires an accurate mathematical model of the underlying process. Unfortunately, most mathematical models are crude abstractions of biological reality and pose unique challenges in control applications [1]. Multiple models currently exist that describe aspects of the TCR-activated signaling pathways that differ in dominant species, network structure, parameter values, and functional representation [2-5]. As with most signaling pathways, the limited amount of pre-existing quantitative data and qualitative observations is unable to unambiguously discriminate between the models.

Multiple models, or scenarios, have been previously used to improve robustness in closed-loop model-based control to parametric uncertainty [6, 7]. Rao *et al*. [8] computed control actions by weighting step-response models using relative Bayesian probabilities to control hemodynamic variables in hypertensive subjects. Kuure-Kinsey *et al*. [9] extended the concepts in [8] for disturbance rejection in a van de Vusse reactor, using an average linear prediction model generated by multiple Bayesian probability-weighted linear models. The recursive weighting system effectively eliminated the "hard switch" between controllers. Noble *et al*. [10] predictably manipulated cell differentiation experimentally with a model predictive controller based on multiple data-consistent parameter characterizations. All of these approaches use feedback that is not available for control of signaling pathways. Furthermore, the limited signaling data do not support Bayesian methods. Consequently, existing techniques for multiple-model control are insufficient for controlling T-cell signaling.

In this paper we present a practical framework for designing open-loop control informed by multiple models for directing intracellular signaling dynamics in T cells. To address model uncertainty, we consider weighted predictions made by multiple nonlinear ordinary differential models of T-cell signaling to design controller actions (manipulations). Prediction model weights are based upon Akaike's Information Criterion (AIC), an information-theoretic method previously used for model selection that considers complexity and fitness to existing experimental data [11, 12]. To facilitate the open-loop controller design, we employ the model predictive control framework. Thus we propose an adaptive Akaike-based multiple-model predictive control for open-loop control of T-cell signaling. This strategy is evaluated using simulated and *in vitro* experiments on a well-established cell line (Jurkat) typically used for studying T-cell signaling pathways.

II. Methods

The control strategy presented herein employs multiple prediction models to form a compromise control sequence that ameliorates the effects of the inaccuracies of any single model. As illustrated in Fig. 1, the first stage is to select an

*Research supported by the National Science Foundation under the grant DMS-09002677.

J. P. Perley is with the Weldon School of Biomedical Engineering, Purdue University, West Lafayette, IN 47906 (email: jperley@purdue.edu).

J. Mikolajczak is with Department of Medicinal Chemistry & Molecular Pharmacology, Purdue University, West Lafayette, IN 47906.

V. C. Dinh is with the Department of Mathematics, Purdue University, West Lafayette, IN 47906.

M. L. Harrison is with the Department of Medicinal Chemistry & Molecular Pharmacology, Purdue University, West Lafayette, IN 47906.

G. T. Buzzard is with the Department of Mathematics, Purdue University, West Lafayette, IN 47906.

A. E. Rundell is with the Weldon School of Biomedical Engineering, Purdue University, West Lafayette, IN 47906 (email: rundell@purdue.edu).

978-1-4673-2066-5/12/$31.00 ©2012 IEEE

appropriate set of prediction models to populate the model bank. Using initial model weights estimated from training data, the multiple-model controller surveys the input space and proposes a control action for the next control update step. Since models differ in accuracy for different scenarios or data sets, model weights are re-estimated using the portion of the training data that most closely corresponds to the proposed control action. Adaptation continues until model weights (and associated control action) no longer change or a maximum iteration is reached. The process repeats for each control update step and continues until the entire open-loop control sequence has been specified and is ready to be applied to the simulated or experimental plant.

A. Model Representation

The multiple-model control strategy is based on the use of a set of mathematical models, $M = \{M^{(1)},...,M^{(n_M)}\}$, of the general form given by (1):

$$M^{(i)} = \begin{cases} \dot{x}^{(i)} = f^{(i)}(x^{(i)},u,\theta^{(i)},t), \; x^{(i)}(t_0) = x_0^{(i)}, \\ y^{(i)} = g^{(i)}(x^{(i)}), \end{cases} \quad (1)$$

where the superscript i denotes the model number. The state variables, manipulated variables (control inputs), process parameters and process outputs are $x \in \Re^n$, $u \in \Re^d$, $\theta \in \Re^p$ and $y \in \Re^m$ respectively, and $f : \Re^n \times \Re^d \to \Re^n$ and $g : \Re^n \to \Re^m$ are twice continuously differentiable functions for process dynamics and outputs, respectively.

B. Prediction Model Bank

The targeted signaling pathway is the TCR-activated extracellular signal-regulated kinase (Erk, or MAPK) pathway as shown in Fig. 2. The engagement of the TCR causes recruitment of protein tyrosine kinase Zap70 and Src-family kinases Lck and Fyn, which initiates signal propagation to the Erk-MAPK cascade. Two ordinary differential equation (ODE) models of the TCR-mediated signaling cascade are used for the basis of the model bank [2, 3] with four additional hybrid models created from these two by replacing the ubiquitous MAPK cascade portion (Fig. 2B) of the signaling pathway with models from Levchenko *et al.* [13]. The Zheng *et al.* [2] model (Z_0) contains primarily first- and second-order mass action kinetics with 24 ODEs and 53 reaction parameters. The Lipniacki *et al.* [3] model (L_0) differs in that it explicitly incorporates SHP-mediated negative feedback and Erk-mediated positive feedback to characterize the kinetic proofreading inherent to the TCR signaling pathway. The model consists of 37 ODEs and 97 parameters derived from mass action kinetics.

To illustrate the controller method with a sufficiently rich set of ODE-based models without additional complications derived from fuzzy logic or Boolean models, we formulated four hybrid models by modifying the Erk-MAPK cascade equations in Z_0 and L_0 with two alternative MAPK models presented by Levchenko *et al.* [13] that employ Michaelis-Menten-derived rate equations with and without the presence of scaffold proteins. The Levchenko model without the

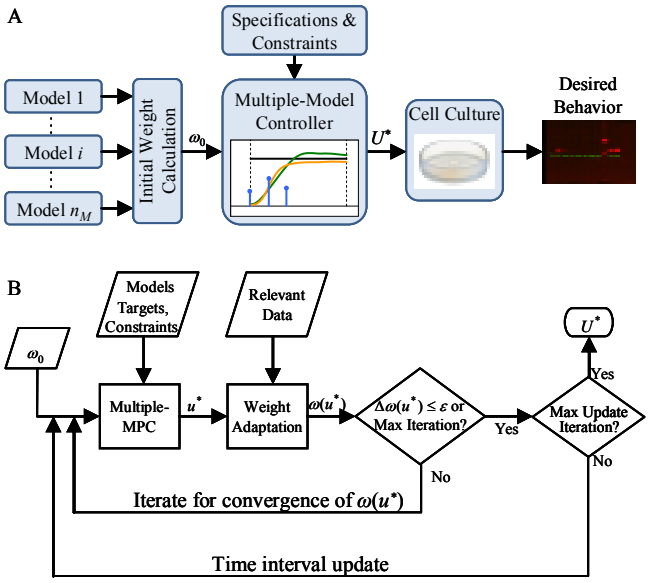

Figure 1. Block diagram of multiple model control strategy. (A) Overview of open-loop configuration for implementation of multiple model-based control of T-cell signaling in the laboratory. (B) Detailed flowchart of adaptive Akaike-weighted multiple-model control algorithm.

scaffold contains 22 ODEs with 30 kinetic parameters while the version with scaffold proteins contains 86 ODEs with 300 parameters. Fig. 2C illustrates how these additional models were formed. We denote these additional models by: Z_0+Scaffold (Z_S), Z_0+No Scaffold (Z_{NS}), L_0+Scaffold (L_S) and L_0+No Scaffold (L_{NS}).

The output of each model is considered to be the total concentration of phosphorylated Erk. The prediction models were modified to contain control inputs that simulate the action of two commercially available reagents that regulate T-cell signaling: sanguinarine and U0126 (shown in Fig. 2 in red). Sanguinarine is an inhibitor of Erk phosphatase and can lead to increased phosphorylation of Erk [14]. U0126 on the other hand is a small molecule inhibitor of Mek with high selectivity [15] which effectively inhibits activation of Erk. For each prediction model, optimal parameter vectors were determined by minimizing the residual sum of squares between model outputs and training data. To account for the differences in scale between the models, the outputs were normalized to ensure that the peak uncontrolled response scaled to unity.

C. Akaike Model Weight Calculation

Using inferences made by multiple competing prediction models with varying levels of accuracy and complexity necessitates the use of a weighting system to rank our confidence in each model. Akaike's Information Criterion (AIC) provides a practical measure of the tradeoff between model fitness and complexity by estimating the theoretical Kullback-Leibler (KL) "distance", or loss of information, between an approximating model and full reality [11]. Denoting the parameter estimates $\hat{\theta}$, given model $M^{(i)}$ and a set of data y, the relative KL information is approximated by the biased log-likelihood function defined by (2):

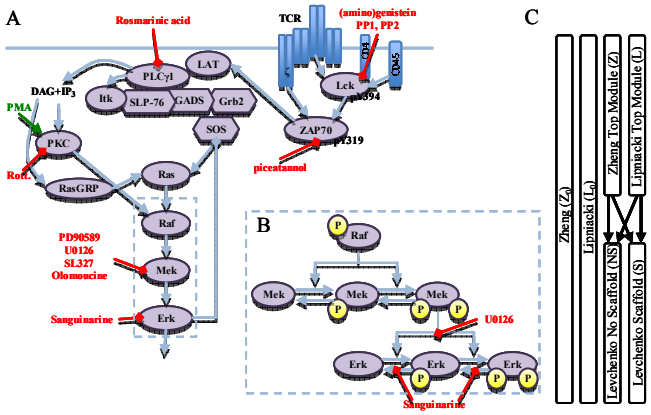

Figure 2. TCR-mediated signaling pathway. (A) General representation of critical components and reactions that are characterized by the prediction models. (B) Expanded view of reaction in the Erk-MAPK cascade. Arrowheads denote activation of target molecule or reaction direction and diamond heads denote inhibition. Molecules in green and red are activators and inhibitors, respectively, and denote possible control reagents. (C) Illustration depicting how modules are combined to form prediction models in the model bank.

$$AIC^{(i)} = -2\log(\ell(\hat{\theta}^{(i)} \mid y)) + 2K\,, \tag{2}$$

where ℓ is the log-likelihood function and K, denoting the number of model parameters, is the bias estimate (the factor 2 was introduced for historical reasons). Assuming normally distributed errors with constant variance, then the AIC can be estimated as (3):

$$AIC^{(i)} = N\log(\varepsilon^{(i)\mathrm{T}}\Lambda^{(i)}\varepsilon^{(i)}/N) + 2K\,, \tag{3}$$

where N is the number of data and $\varepsilon^{(i)} = [y_1^{(i)} - y_1^{exp},\ldots,y_N^{(i)} - y_N^{exp}]^{\mathrm{T}}$ is the vector of residuals between experimental data y^{exp} and their corresponding outputs $y^{(i)}$ from the i^{th} model. The residual weighting matrix, $\Lambda^{(i)}$, is traditionally the identity although herein we will use it to selectively weight models and subsets of the data as further explained in Section E.

If $N/K < 40$, an additional bias term is introduced to accommodate small samples to yield the corrected-AIC (AICc) given by (4):

$$AICc^{(i)} = AIC^{(i)} + \frac{2K(K+1)}{N-K-1}\,. \tag{4}$$

It is important to note that the AICc values are only meaningful relative to one another. This stems from the AIC being a relative rather than absolute estimate of KL distance. As a result, only the quantity $\Delta^{(i)} = AICc^{(i)} - AICc_{\min}$ will be considered for each model. It follows that the relative likelihoods of the models are given by the Akaike weights, given by (5):

$$\omega^{(i)} = \frac{\exp(-\Delta^{(i)}/2)}{\sum_{j=1}^{n_M}\exp(-\Delta^{(j)}/2)}\,. \tag{5}$$

The weight $\omega^{(i)}$ is considered to be the strength of evidence in support of the i^{th} model being the KL best model given the data and the set of models [11].

D. Akaike-Weighted Multiple-Model Predictive Control

The multiple-model control strategy is built around the conventional MPC framework in order to reduce the computational complexity of the open-loop control problem. At each update index, the controller surveys the possible trajectories stemming from the current state over a finite prediction horizon (H_p) and control horizon (H_u) and selects the control sequence so that the predicted output tracks a desired trajectory. The initial value of the control sequence is set and used to update the states of the prediction models so the procedure can repeat for the remaining control update steps.

The control objective function penalizes the error between the predicted output for model i and the desired trajectory and a measure of the control effort over the prediction horizon starting at time $t_k \in T_s$, as given by (6):

$$J^{(i)}(U) = [Y^{(i)} - S]^{\mathrm{T}} Q[Y^{(i)} - S] + U^{\mathrm{T}} RU\,, \tag{6}$$

where the vectors $Y^{(i)} = [y_1^{(i)}(t_{k|k}),\ldots,y_m^{(i)}(t_{k+H_p|k})]^{\mathrm{T}}$ and $S = [s_1(t_k),\ldots,s_m(t_{k+H_p})]^{\mathrm{T}}$ are the predicted and target outputs over H_p, respectively, $U = [u_1(t_{k|k}),\ldots,u_d(t_{k+H_u-1|k})]^{\mathrm{T}}$ are the discrete controller inputs over H_u, and Q and R are diagonal weighting matrices associated with the error and control effort, respectively.

The optimal control sequence is determined by solving the optimization problem posed in (7):

$$\begin{aligned} U^* = \arg\min_{U}\ & \omega(U)^{\mathrm{T}} J(U) \\ \text{s.t.}\ \ & U_{\min} \le U \le U_{\max}\,, \end{aligned} \tag{7}$$

where ω and J are vectors of Akaike weights and objective function values associated with the n_M prediction models. Thus the control objective minimizes a weighted aggregate of the predictions from multiple models that mitigates the inaccuracies of any single model. Herein, the solution to (7) is computed by MATLAB's constrained nonlinear optimization solver (*fmincon*).

E. Akaike Model Weight Adaptation

As illustrated in Fig. 1, model weights, computed using (3)-(5), are updated from their original values based on the proposed control action at each step. Primarily due to the effects of model-plant mismatch, it is quite common for a model's fitness quality to change between data sets generated under different experimental conditions (i.e. different levels or combinations of the control inputs). Therefore, we adaptively update the Akaike weights to consider only the training data collected under conditions that most closely resemble the proposed control action.

For a given number of training data sets, let $u_{k,j}$ be the input used to generate the observations $y_{k,j}^{exp}$ for the j^{th} experiment involving the k^{th} control variable. Furthermore, let u_k^* be the proposed control action for the k^{th} control variable at the current update step. For the following calculations, the magnitudes of $u_{k,j}$ and u_k^* should be

normalized by their corresponding upper bounds to prevent giving disproportionate weight to larger values. The relative distance between the points on the input space and the predicted control action in the k^{th} dimension is $\delta_{k,j} = |u_{k,j} - u_k^*|$. Now, let us only consider the points in each dimension that neighbor u_k^* since they most directly correspond to the current proposed control action. Let R_k refer to these points, that is, the set of indices of two points in the k^{th} dimension forming the smallest interval containing u_k^*. This leads to the relative weight of each point in R_k with respect to u_k^* defined by (8):

$$\alpha_{k,r} = 1 - \frac{\delta_{k,r}}{L_k}, \tag{8}$$

for r in R_k, where L_k is the distance between the two points in R_k. Now, the residuals between the observations $y_{k,r}^{exp}$, where $r \in R_k$, and the corresponding outputs predicted by each model under the same conditions will be weighted by the term denoted by (9):

$$\beta_{k,r} = \frac{u_k^*}{\sum_{q=1}^{d} u_q^*} \alpha_{k,r}, \tag{9}$$

where d is the dimension of the input space. The term $\beta_{k,r}$ is used to weight the residuals computed from data generated under experimental conditions most similar to the proposed control action. We use the weights in (9) as the entries in a diagonal matrix, Λ, to be used as the residual weighting matrix in (3). The corresponding residual is the vector of differences, $y_{R_k}^{(i)} - y_{R_k}^{exp}$, over the corresponding set of R_k and i. Using updated definitions for Λ and $\varepsilon^{(i)}$ to only include the subset of relevant data, new Akaike weights are computed using (3)-(5). In essence, this adaptive weighting strategy gives priority to the models best supported by the data relevant to the experiment at hand in the calculation of the Akaike weights for the next iteration.

F. Experimental Methods

Erk phosphorylation (pErk) data were collected from Jurkat T leukemia cell line (Jurkat clone E6.1; ATCC). Cells were grown in RPMI 1640 (Sigma) supplemented with 7.5% heat-inactivated fetal bovine serum (BioWest), 1mM sodium pyruvate (Gibco), 12.5 mM HEPES pH 7.4 (Sigma), 12 μM sodium bicarbonate (Sigma) 50 μM 2-Mercaptoethanol (Sigma), 50 μg/ml streptomycin and 50 units/ml penicillin in an incubator at 37ºC in humidified air containing 5% carbon dioxide. Cells were harvested in log-phase growth and 2 x 10^7 cells per treatment. Cells were stimulated using anti-human CD3 (10 μg/ml, clone: UCHT-1, eBioscience) as the stimulatory signal at 37ºC in a water bath. Cells were treated with the Mek1/2 inhibitor U0126 (Calbiochem) or the MKP inhibitor sanguinarine (Sigma), depending on the protocol, dissolved in DMSO at the indicated time points with the indicated concentrations. Experimental control samples where treated with the same amount of DMSO. Samples of 2 x 10^6 cells were taken at the indicated time points and lysed in 1% NP40 lysis buffer (1% NP40, 25 mM Tris, pH 7.4, 150 mM NaCl, 5 mM EDTA, 1mM NaV, 10 mM NaF, 10 μg/ml each of aprotinin and leupeptin) for 15 min on ice. Lysates were centrifuged for 5 min at 18000 g at 4ºC. The supernatant was added to the same volume of 2X protein solubilizing mixture (PSM, 25% (w/v) sucrose, 2.5% (w/v) sodium dodecyl sulfate, 25 mM Tris, 2.5 mM EDTA, 0.05% bromophenol blue) and boiled for five minutes. Proteins were separated via SDS-PAGE, blotted for phospho-Erk1/2 (Cell Signaling), phospho-ZAP-70 (pY319, Cell Signaling) and GAPDH (Ambion). IRDye 800 and 680 secondary anti-mouse and anti-rabbit antibodies (Li-Cor) were used for signal detection using an Odyssey infrared scanner. Images of the blots were analyzed using ImageJ to produce quantitative data for model comparison. Model predictions were scaled to compensate for the fact that the data showed relative quantities only rather than absolute concentrations.

III. Results and Discussion

The performance of the open-loop multiple-model control strategy for systematically manipulating T-cell signaling dynamics is evaluated using two approaches: simulated experiments and laboratory experiments. For simulated experiments, the controller is trained with data generated from *in silico* experiments to demonstrate the effectiveness of the multiple-model controller and adaptive weighting strategy. For laboratory experiments, the open-loop control sequence is administered to a population of Jurkat T cells to evaluate its ability to direct TCR-mediated signaling *in vitro*. For this case, training data were also collected from *in vitro* experiments. In both cases, the training experiments were designed to rapidly screen the effects of the control reagents on a T cell population (*in silico*: n = 3; *in vitro*: n = 1). In all there were 10 experiments: four different doses of sanguinarine (5, 10, 20 and 50 μM), five different doses of U0126 (0.5, 1, 2, 5 and 10 μM), and an experimental control (i.e. no inputs). Control inputs were added at 5 minutes after stimulation by anti-CD3 and samples of pErk were taken at 0, 2, 5, 10, 12, 15, 20 and 30 minutes.

For both the simulated and laboratory experiments, the desired trajectory (target profile) for the model output is defined by the equation $s_1(t) = (1 - e^{-t})(1 + e^{t-10})^{-1}$. It has been reported that constitutive activation of the Erk pathway is present in high frequency (>50%) in patients suffering from acute myeloid leukemia (AML) and is associated with a marked reduction in survival duration [16, 17]. This suggests it may be therapeutic to rapidly force pErk to baseline levels shortly after reaching its peak activity as defined by s_1. Manipulated variables u_1 and u_2 are defined to be concentrations of sanguinarine and U0126, respectively. The five possible input update steps (dosing times) T_s begin at 3 minutes post-stimulation with anti-CD3 and are spaced 5 minutes apart to accommodate both the rapid dynamics of TCR signaling and the experimental constraints on input update and observation rates. The experiment is terminated at 30 minutes when no inputs are applied but measurements

are taken. The horizons H_u and H_p are set to 1 and 2, respectively, and weighting matrices Q and R are each chosen to be identity. Input constraints on sanguinarine and U0126 are set to $[0, 50]\,\mu M$ and $[0, 10]\,\mu M$, respectively. The rationale for the upper limits come from experimental results that indicate saturation effects at levels above the specified concentrations.

A. Simulated Controller Performance

In the simulated case, the multiple-model controller is evaluated six different times, each time assuming a different model as the "true" but unknown plant. Noisy data are generated from the "true" plant model using the conditions described in the previous section and adding 10% Gaussian noise. For each simulated data set in triplicate, all six prediction models are re-fitted to the data and new model weights are computed using (3)-(5). For illustrative purposes, only two simulated experiments are shown: (1) Z_0 as the "true" plant and (2) L_{NS} as "true" plant. It is evident from Fig. 3A,D that the accuracy of the prediction models partially depends on the training data. In the case where the Z_0 plant is assumed, the Akaike weights strongly favor the predictions from the Z_0 model. This suggests that its predictive capability is unmatched by rival models given the available data. However, when the L_{NS} plant is assumed, the weights tended to oscillate between L_{NS} and L_0, most likely due to the number of shared characteristics between the two structures. This also suggests that the predictive capacity of both models changed as a function of the control input updates. As it is unclear which is more favorable, both models are used to inform the controller. In both cases the adaptive weighting strategy is able to filter out unlikely models given the training data. As shown in Fig. 3B,E the controller chose a ramp-up in U0126 doses between 8 and 13 minutes for the scenario when Z_0 was the "true" but unknown plant, while a single bolus-type dose was chosen for the L_{NS} plant scenario. Nevertheless, the plant output tracked the target response reasonably well even though the two predicted control actions were different (Fig. 3C,F). This is in stark contrast to the performances of single-model controllers with similar MPC set-ups (Fig. 4). When the plant and prediction model are mismatched, a likely scenario in practice, there is moderate to extreme deterioration in the tracking performance (e.g. when Z_{NS} informs the controller).

B. Experimental Controller Performance

Training data were collected according to Sections IIF and III. The addition of low to moderate doses of sanguinarine had negligible effects on pErk concentrations. Only the highest dose tested caused a sustained elevation of pErk. On the other hand, U0126 produced immediate reductions in pErk concentrations even at low doses. The representation of the controller input functions in the prediction models were modified to exhibit these trends.

Starting with the training data, the multiple-model open-loop control strategy with adaptive Akaike weights is implemented to evaluate its ability to direct TCR-mediated

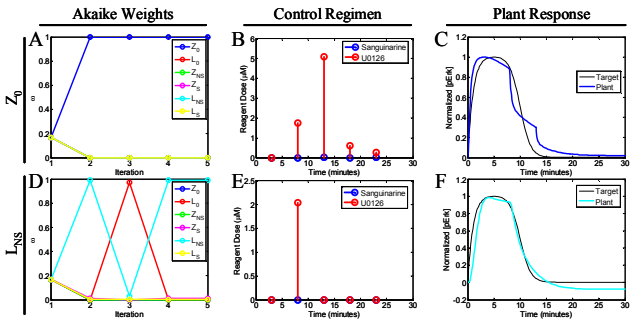

Figure 3. Illustrative results of *in silico* controller implementation. Row labels denote the prediction models used to generate training data (with 10% Gaussian noise added). (A, D) Akaike weight adaptation for all models. (B, E) Control sequence computed by the controller considering all six prediction models fitted to simulated data. (C, F) Normalized pErk concentration of the plant with multiple model informed open loop control. Note that a negative value means that the output is below its initial concentration.

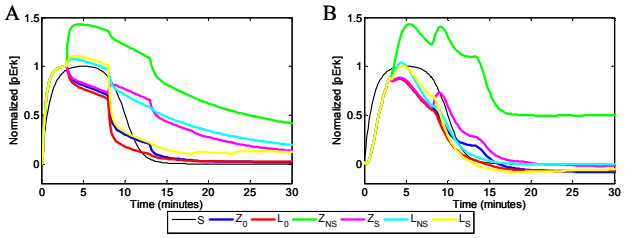

Figure 4. *In silico* single-model controller performance. Predicted pErk dynamics for assumed plants (A) Z_0 and (B) L_{NS}. Legend denotes prediction model used to inform the controller and resulting plant output.

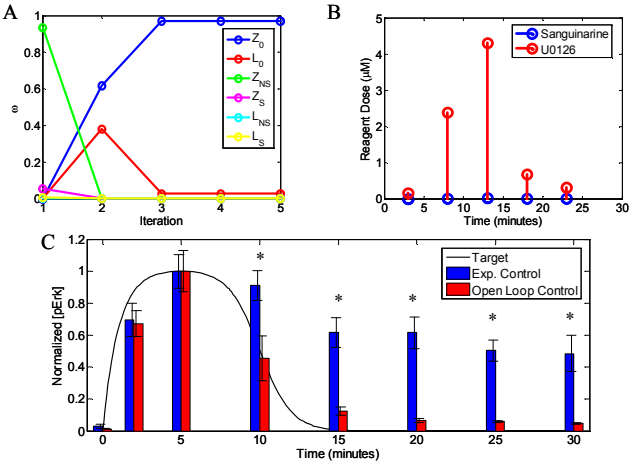

Figure 5. Results of *in vitro* controller implementation. (A) Akaike weight adaptation for all prediction models. (B) Control sequence computed by the controller considering all six prediction models fitted to *in vitro* training data. (C) Normalized *in vitro* pErk concentrations collected from the experimental control (i.e. no inputs) shown in blue and the multiple-model open-loop control-based experiment shown in red (n=3 for both sets). Asterisks (*) denote statistically significant differences between groups ($p<0.05$) as calculated by one-way ANOVA with Tukey multiple comparisons test. Data shows mean ± standard error.

signaling *in vitro*. Comparing Fig. 5A with Fig. 3A reveals an interesting contrast between the cases of model training with experimental data as opposed to simulated data. Initially, Z_{NS} vastly outweighs its rivals, resulting in a control strategy based primarily on it alone. As the open-loop

control sequence is being built, however, there is a dramatic shift in confidence towards Z_0, indicating it is a better fit to the relevant data collected under conditions at each of the subsequent controller update steps. Had a single prediction model or a fixed weighting strategy been used, one could not be as confident in the resulting controller given the data. This demonstrates that the models' predictive capabilities can be variable over the input space especially when training data is limited and noisy. Furthermore, this supports the usefulness of the adaptive Akaike weights in the open-loop multiple-model control problem. When implemented in the laboratory, the proposed control sequence (shown in Fig. 5B) was able to effectively drive the relative levels of pErk along the target trajectory (n = 3, shown in Fig. 5C).

IV. Conclusion and Future Work

This work presents a practical framework for open-loop control of uncertain nonlinear systems using multiple models to generate predictable dynamical responses. The model weighting strategy employs adaptive Akaike weights that give priority to the models most supported by the data relevant to the control input at that update step. This open loop controller design pairs multiple model predictive control with adaptive Akaike model weights to create a cohesive strategy for systematically utilizing the most relevant knowledge embedded within limited training data in a computationally tractable manner.

In silico controller implementation showed excellent performance in tracking a target response profile despite the uncertainty from multiple model characterizations. These results were corroborated with *in vitro* experiments. However, the precision gained by using multiple prediction models came at the expense of computational efficiency. The computation time is approximately proportional to the number of models and iterations of the weight adaptation algorithm, with variability due to the complexity of the additional models and the modified objective space topography. The proposed approach also does not incorporate new data in real time. Unfortunately, the maximum feedback frequency afforded by current experimental protocols is insufficient to control the rapid dynamics of Erk signaling. Open-loop control provides the only reasonable systematic means of manipulating Erk dynamics. That said, one could easily modify the proposed approach to accommodate observational feedback should it be available.

Future work will emphasize cost manifold identification for accurate and efficient solution to the multiple-model predictive control problem. Incorporating parametric uncertainties will be streamlined to better inform the design of compromise solutions. Next steps will also address multi-output control to systematically manipulate the dynamics of more than one signaling species within a signaling pathway to allow for more sophisticated control strategies.

The TCR Erk-MAPK signaling pathway studied herein is known to be associated with allergies, asthma, auto-immune disorders, and acute myeloid leukemia among others [16, 17]. The ability to predictably alter the T-cell signal transduction dynamics, and thereby indirectly modify the transcription factor activation profile and gene regulatory networks, may ultimately have therapeutic applications.

References

[1] E. D. Sontag, "Molecular systems biology and control," *European Journal of Control,* vol. 11, pp. 396-435, 2005.

[2] Y. Zheng and A. Rundell, "Comparative study of parameter sensitivity analyses of the TCR-activated Erk-MAPK signalling pathway," *IEEE Proceedings Systems Biology,* vol. 153, pp. 201-211, Jul 2006.

[3] T. Lipniacki, B. Hat, J. R. Faeder, and W. S. Hlavacek, "Stochastic effects and bistability in T cell receptor signaling," *Journal of Theoretical Biology,* vol. 254, pp. 110-122, Sep 2008.

[4] J. Saez-Rodriguez, L. Simeoni, J. A. Lindquist, R. Hemenway, U. Bommhardt, B. Arndt*, et al.*, "A logical model provides insights into T cell receptor signaling," *Plos Computational Biology,* vol. 3, pp. 1580-1590, Aug 2007.

[5] A. Saadatpour, R.-S. Wang, A. Liao, X. Liu, T. P. Loughran, I. Albert*, et al.*, "Dynamical and Structural Analysis of a T Cell Survival Network Identifies Novel Candidate Therapeutic Targets for Large Granular Lymphocyte Leukemia," *Plos Computational Biology,* vol. 7, Nov 2011.

[6] R. Huang and L. T. Biegler, "Robust nonlinear model predictive controller design based on multi-scenario formulation," in *2009 American Control Conference, Vols 1-9*, ed New York: IEEE, 2009, pp. 2341-2342.

[7] P. Falugi, S. Olaru, and D. Dumur, "Robust Multi-model Predictive Control Using LMIs," *International Journal of Control Automation and Systems,* vol. 8, pp. 169-175, Feb 2010.

[8] R. R. Rao, B. Aufderheide, and B. W. Bequette, "Experimental studies on multiple-model predictive control for automated regulation of hemodynamic variables," *Ieee Transactions on Biomedical Engineering,* vol. 50, pp. 277-288, Mar 2003.

[9] M. Kuure-Kinsey and B. W. Bequette, "Multiple Model Predictive Control of Nonlinear Systems," *Nonlinear Model Predictive Control: Towards New Challenging Applications,* vol. 384, pp. 153-165, 2009.

[10] S. L. Noble, L. E. Wendel, M. M. Donahue, G. T. Buzzard, and A. E. Rundell, "Sparse-Grid-Based Adaptive Model Predictive Control of HL60 Cellular Differentiation," *IEEE transactions on bio-medical engineering,* vol. 59, pp. 456-63, 2012-Feb 2012.

[11] K. P. Burnham and D. R. Anderson, *Model Selection and Multimodel Inference: A Practical Information-Theoretic Approach*, 2nd ed. New York: Springer-Verlag, 2002.

[12] M. J. Dunlop, E. Franco, and R. M. Murray, "A multi-model approach to identification of Biosynthetic pathways," in *American Control Conference 2007*, New York, NY, 2007, pp. 3493-3498.

[13] A. Levchenko, J. Bruck, and P. W. Sternberg, "Scaffold proteins may biphasically affect the levels of mitogen-activated protein kinase signaling and reduce its threshold properties," *Proceedings of the National Academy of Sciences of the United States of America,* vol. 97, pp. 5818-5823, May 2000.

[14] A. Vogt, A. Tamewitz, J. Skoko, R. P. Sikorski, K. A. Giuliano, and J. S. Lazo, "The benzo c phenanthridine alkaloid, sanguinarine, is a selective, cell-active inhibitor of mitogen-activated protein kinase phosphatase-1," *Journal of Biological Chemistry,* vol. 280, pp. 19078-19086, May 2005.

[15] M. F. Favata, K. Y. Horiuchi, E. J. Manos, A. J. Daulerio, D. A. Stradley, W. S. Feeser*, et al.*, "Identification of a novel inhibitor of mitogen-activated protein kinase kinase," *Journal of Biological Chemistry,* vol. 273, pp. 18623-18632, Jul 1998.

[16] M. R. Ricciardi, T. McQueen, D. Chism, M. Milella, E. Estey, E. Kaldjian*, et al.*, "Quantitative single cell determination of ERK phosphorylation and regulation in relapsed and refractory primary acute myeloid leukemia," *Leukemia,* vol. 19, pp. 1543-1549, Sep 2005.

[17] S. M. Kornblau, M. Womble, Y. H. Qiu, C. E. Jackson, W. J. Chen, M. Konopleva*, et al.*, "Simultaneous activation of multiple signal transduction pathways confers poor prognosis in acute myelogenous leukemia," *Blood,* vol. 108, pp. 2358-2365, Oct 2006.